Solid-state NMR and DNP Investigations of Carbohydrates and Cell-wall Biomaterials

Liyanage D. Fernando[1], Wancheng Zhao[1], Malitha C. Dickwella Widanage[1], Frédéric Mentink-Vigier[2] & Tuo Wang[1]

[1] *Louisiana State University, Baton Rouge, LA, USA*
[2] *National High Magnetic Field Laboratory, Tallahassee, FL, USA*

The cell walls in plants and microbes serve as a central source for biorenewable energy and biomaterials, as well as the target for novel antibiotics and antifungals. They are biocomposites abundant in complex carbohydrates, a class of biologically important but underinvestigated molecules. Solid-state nuclear magnetic resonance (ssNMR) of carbohydrate materials and cell walls has made significant progress over the past 10 years. This article summarizes the recent ssNMR studies that have elucidated the polymorphic structure and heterogeneous dynamics of polysaccharides and other biomolecules, such as proteins, lignin, and pigment, in the intact cell walls or biofilms of 11 species across plants, fungi, bacteria, and algae. We also highlight the assistance of magic-angle spinning dynamic nuclear polarization (MAS-DNP) in the enhanced detection of the interaction interface involving lowly populated biopolymers and summarize the recent applications of natural-abundance MAS-DNP in cell-wall research, which could substantially broaden the scope of biomolecular NMR by skipping isotope labeling.

Keywords: solid-state NMR, MAS-DNP, carbohydrate, cell wall, polymer

How to cite this article:
eMagRes, 2020, Vol 9: 251 – 258. DOI 10.1002/9780470034590.emrstm1624

Introduction

Complex carbohydrates are a class of fundamental biomolecules that are spectroscopically difficult to handle. This is because the basic structures of the constituent monosaccharide units are similar, but the polymerized macromolecules are highly polymorphic due to the significant variations in the covalent linkage, torsional conformation, chemical substitution, and hydrogen bonding network. The structural complexity is further enhanced when these polysaccharides are placed in the cell wall and assembled with other biopolymers. Since carbohydrates are crucial to cellular signaling and recognition, energy storage, and structural building, and the cell walls are the central sources for biofuel and biomaterial production, there is a strong need for establishing a nondestructive and high-resolution method to elucidate the structure and dynamics of polysaccharides and the architecture of their supramolecular composites.

For decades, magic-angle spinning (MAS) solid-state nuclear magnetic resonance (ssNMR) has been widely employed to elucidate the structural polymorphism of native and engineered carbohydrates. At the early stages, 1D ^{13}C ssNMR is the primary technique for distinguishing the magnetically nonequivalent glucose units in the Iα, Iβ, and other allomorphs of the highly crystalline cellulose.[1] Molecular insights have also been obtained to estimate the relative crystallinity and the number of glucan chains in cellulose microfibril by quantifying the intensity ratio between the peaks of surface and interior glucan chains, as well as to probe the polymer distribution in mobile or rigid domains of plant cell walls by measuring relaxation-filtered spectra.[2,3] Most of these studies are focused on isolated and purified carbohydrate components or specialized cell walls that are rich in certain carbohydrate components, and the limitations in resolution and sensitivity have made it difficult to investigate the more complicated whole-cell systems.

Recently, by combining multidimensional correlation techniques, high magnetic fields, and isotope labeling, it becomes possible for us to resolve the sophisticated structure and packing of carbohydrates in their cellular environment and explore their functional relevance to material properties. The spectroscopic methods mainly include a series of through-space (CORD, DARR, RFDR, PAR, CHHC, etc.) and through-bond (J-INADEQUATE, INEPT, etc.) correlation methods that allow for resonance assignment and determination of covalent linkages or spatial proximities,[4–7] measurements of relaxation and dipolar couplings for understanding polymer dynamics, water-editing experiments for probing water accessibility,[8,9] dipolar- or paramagnetic-based distance measurements for determining ligand-binding (REDOR, PRE, etc.),[10,11] sensitivity-enhancing DNP methods for magnifying the signals of minor species,[12–14] and spectral-editing techniques for lightening the spectral crowding issue in whole-cell studies.[15,16]

These ssNMR measurements are often coupled with supplementary biochemical techniques. For example, the *de novo* assignment of polysaccharide signals is usually validated

by involving the genetic mutants or chemically treated samples that specifically knock out certain carbohydrate components.[17–20] The polymer structure and molecular composition derived using NMR chemical shifts and peak intensities are typically compared with the results from the biochemical analyses of glycosyl composition and linkage patterns.[21,22]

This established spectroscopic and biochemical toolbox has substantially promoted high-resolution carbohydrate ssNMR studies over the past decade: among the 450 compounds indexed by Complex Carbohydrate Magnetic Resonance Database (CCMRD),[23] 312 entries are from publications after 2010. This article selectively discusses the key findings and technical innovations of recent ssNMR studies on the cell-wall biomaterials from model plants (*Arabidopsis thaliana, Brachypodium distachyon, Zea mays*, poplar, and spruce), fungal pathogens (*Aspergillus fumigatus* and *Cryptococcus neoformans*), bacteria (*Escherichia coli* and *Bacillus subtilis*), and microalgae (*Chlamydomonas reinhardtii*). We also discuss how cell-wall research has been benefited from the development of magic-angle spinning dynamic nuclear polarization (MAS-DNP) methods and emphasize the new research opportunities enabled by natural-abundance DNP.

Solid-state NMR Investigations of Cell Walls in Plants, Fungi, Bacteria, and Algae

Polysaccharide Networks and Protein-mediated Loosening of Primary Plant Cell Walls

Since 2011, Hong and coworkers have been employing a series of 2D/3D ssNMR techniques to elucidate the packing of polysaccharides in uniformly ^{13}C-labeled primary plant cell walls (grown using $^{13}CO_2$ or ^{13}C-glucose) and the mechanism through which a class of functional protein (expansin) unlocks the polysaccharide networks for cell expansion.[24] The primary cell wall being studied is a component synthesized during plant growth; it is mainly a composite of three types of polysaccharides: the partially crystalline cellulose microfibrils that are formed by 18 or more glucan chains (3–4 nm across), the hemicellulose that interacts with cellulose microfibrils, and the acidic pectin that regulates cell-wall hydration and porosity. Multiple model plants have been investigated, including the intact cell walls as well as the chemically/enzymatically digested residuals of *Arabidopsis*, *Brachypodium*, and maize. A more detailed discussion of these studies can be found in Reference 24, and here we only briefly highlight three major contributions. First, the spectral resolution on high-field magnets (0.7 ppm on 800 MHz) is sufficient for unambiguously resolving the seven types of glucose units that coexist in a cellulose microfibril, determining their hydroxymethyl torsional conformation through ^{1}H–^{1}H distance measurements, and mapping out their relative location within a microfibril.[25,26] Second, a systematic investigation of polymer packing, mobility, and hydration using intact, extracted, wild-type, and mutant samples has demonstrated that at least 25–50% of cellulose surface is in subnanometer contact with pectin, which has revised the long-standing concept where these two polymers are phase separated.[27–32] Third, two novel techniques that rely on MAS-DNP and paramagnetic methods have been developed to determine protein–carbohydrate binding in cell walls.[33,34] The protein expansin is found to perturb the cellulose–xyloglucan junctions in *Arabidopsis* (a dicot) but disrupts the connections of highly and lowly substituted glucuronoarabinoxylan in maize (a commelinid monocot); therefore, expansins bind different carbohydrates in compositionally distinct cell walls for function. These molecular insights have been integrated with many biochemical, modeling, and spectroscopic studies[35–38] to substantially advance our understanding of primary cell walls and the structural aspects underlying plant growth.

Lignin–carbohydrate Interactions in Secondary Plant Cell Walls

Inspired by the impactful studies of primary cell walls, recent efforts have been devoted to characterizing the secondary plant cell wall, which is a component synthesized once the cell ceases expansion and forms the majority of the lignocellulosic biomass. The secondary cell wall contains an aromatic polymer named lignin and multiple classes of polysaccharides such as cellulose and the hemicellulose xylan in either twofold (two residues per helical turn; flat ribbon) or threefold (three residues for a 360° fold; nonflat) helical screw symmetry (Figure 1a, left). Benefited from the distinct chemical structures and torsional conformations, the ^{13}C signals of these biomolecules are well resolved in 2D correlation spectra (Figure 1b,c). Dupree and colleagues have conducted a series of 2D and 3D CCC experiments on *Arabidopsis* secondary cell walls, which have revealed that only the flat xylan with a regular pattern of acetate or glucuronate substitutions can bind cellulose.[18,42,43] We have further elucidated how carbohydrates interact with lignin, which is a key interaction that determines the biomass recalcitrance to enzymatic treatment and limits the efficiency of biofuel production. Using multiple model plants, such as *Arabidopsis* and maize, we have identified 234 intermolecular cross peaks that pinpoint subnanometer packing, 325 relaxation curves that probe polymer mobilities, and 62 site-specific data that identify site-specific water interactions of biomolecules, which resolved a unique cell-wall architecture: xylan is bridging the lignin nanodomains (through its nonflat conformers) to cellulose (through its flat-ribbon form) in a conformation-dependent manner.[39] Considering the large chemical shift anisotropy of aromatics, a 600 MHz NMR, instead of higher magnetic fields, is chosen to simultaneously guarantee sufficient resolution and sensitivity.

This structural frame does not apply to all plant species. In 2019, Dupree and colleagues have found that in the softwood spruce, both xylan and galactoglucomannan (GGM, a uniquely abundant hemicellulose in softwood) experience a two-domain distribution, with one domain in contact with cellulose and the other one filling the interfibrillar space.[19] It is thus proposed that some GGM and xylan bind to the same cellulose microfibrils, with lignin in association with these cellulose-bound polysaccharides, apparently, plant species with distinct biopolymer composition expect different cell-wall architectures; there are multiple ongoing projects attempting to

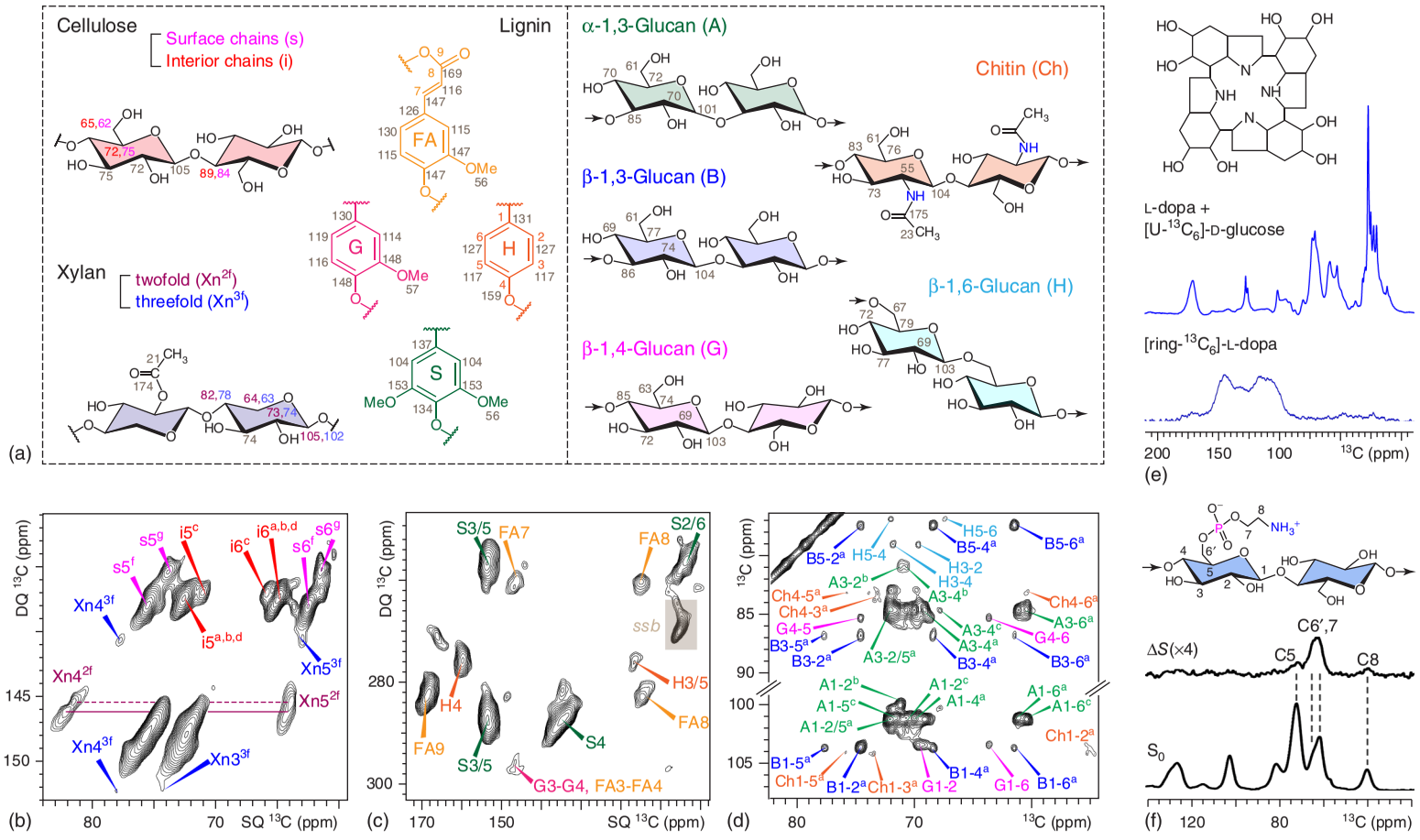

Figure 1. Representative ^{13}C spectra and structures of cell-wall molecules. (a) Typical biomolecules in secondary plant cell walls (left) and fungi (right). The NMR abbreviations are in parenthesis or annotated on the structure, with representative chemical shift values labeled. The 2D ^{13}C INADEQUATE spectra of (b) carbohydrates and (c) lignin are shown for maize stem. (d) 2D ^{13}C–^{13}C CORD spectrum of *A. fumigatus* fungus. Superscripts annotate different conformers. (e) Proposed molecular structures of melanin and 1D ^{13}C CP spectra for *C. neoformans* prepared with natural-abundance L-dopa and [U-$^{13}C_6$]-D-glucose (top) and [ring-$^{13}C_6$]-L-dopa (bottom). (f) Phosphoethanolamine cellulose produced in *E. coli* as revealed by ^{13}C {^{31}P}REDOR. S_0, full-echo spectrum; ΔS, difference spectrum.[22,39–41] ((a) Kang, X., Kirui, A., Muszyński, A., Widanage, M. C. D., Chen, A., Azadi, P., Wang, P., Mentink-Vigier, F., Wang, T. (2018). Molecular architecture of fungal cell walls revealed by solid-state NMR. Nature Communications, 9(1). doi:10.1038/s41467-018-05199-0 and Kang, X., Kirui, A., Dickwella Widanage, M. C., Mentink-Vigier, F., Cosgrove, D. J., & Wang, T. (2019). Lignin-polysaccharide interactions in plant secondary cell walls revealed by solid-state NMR. Nature Communications, 10(1). doi:10.1038/s41467-018-08252-0. Licensed under CCBY 4.0; (b–d) Kang, X., Kirui, A., Dickwella Widanage, M. C., Mentink-Vigier, F., Cosgrove, D. J., & Wang, T. (2019). Lignin-polysaccharide interactions in plant secondary cell walls revealed by solid-state NMR. Nature Communications, 10(1). doi:10.1038/s41467-018-08252-0. Licensed under CCBY 4.0; (e) Chatterjee, S., Prados-Rosales, R., Itin, B., Casadevall, A., & Stark, R. E. (2015). Solid-state NMR Reveals the Carbon-based Molecular Architecture of *Cryptococcus neoformans* Fungal Eumelanins in the Cell Wall. Journal of Biological Chemistry, 290(22), 13779–13790. © 2015. Reprinted with permission from The American Society for Biochemistry and Molecular Biology, Inc; (f) Thongsomboon, W., Serra, D. O., Possling, A., Hadjineophytou, C., Hengge, R., & Cegelski, L. (2018). Phosphoethanolamine cellulose: A naturally produced chemically modified cellulose. Science, 359(6373), 334–338. doi:10.1126/science.aao4096. © 2018 Reprinted with permission from American Association for the Advancement of Science)

reveal the assorted schemes of polysaccharides–lignin assembly in a variety of plant species.

Due to the highly complex nature of these whole-cell systems, ssNMR could not provide a high-resolution structure as for the studies of purified proteins or nucleic acids. However, the conceptual schemes of cell-wall structures derived from the substantive, molecular evidence have already presented a major improvement from the prevailing models purely based on biochemical assays that either substantially perturb the cellular environment or lack the subnanometer resolution to probe the intermolecular contacts between biomolecules.

The Carbohydrate Armor and Pigment Deposition of Fungal Pathogens

In 2018, we have initiated a project to investigate the cell walls of fungal pathogens. These microbes cause invasive infections to more than two million patients annually, with high mortality. The fungal cell wall is of high biomedical significance as it is a major target for antifungal agents (e.g., caspofungin), and this carbohydrate-rich armor confers the fungi with mechanical strength and structural flexibility to survive through external stress. The fungal cell wall contains 50–60% glucans, 20–30% glycoproteins, and a small portion of chitin (Figure 1a, right), and these molecules exhibit beautiful resolution in native, never-dried, and living *A. fumigatus*: on an 800 MHz NMR, the ^{13}C linewidths are 0.5–0.7 ppm for rigid components (Figure 1d) and 0.3–0.5 ppm for mobile molecules.[22] This allows us to resolve the signals of 23 conformers from 7 major types of polysaccharides. Notably, on the world-record 1.5 GHz (35 T) NMR,[44] the ^{13}C resolution has been further improved to 0.3–0.5 ppm even for the rigid molecules, providing a magnified view of structural polysaccharides (unpublished results).

Because α-1,3-glucans are partially extractable using alkali, they have long been assumed an insignificant role in cell-wall mechanics,[45] but they exhibit tens of intermolecular cross peaks with chitin microfibrils in long-range ^{13}C–^{13}C proton-assisted recoupling (PAR) spectra.[22] This unexpected observation echoes the limited water accessibility and low mobility consistently observed in both molecules, and for the first time reveals that the mechanical scaffold of *A. fumigatus* cell wall is formed by tightly packed α-1,3-glucan and chitin. These highly hydrophobic and rigid cores are enclosed within a well-hydrated and dynamic matrix of β-glucans and further capped by an outermost layer that is rich in glycoproteins. With this structural frame, we are currently identifying the structural features that contribute to fungal virulence and drug resistance.

Besides polysaccharides and glycoproteins, fungi also contain a natural pigment named melanin. Stark and coworkers have been tracking down the biosynthesis pathway and molecular structure of melanin, as well as its interactions with carbohydrate components in *C. neoformans* cell walls.[40,46–48] The incorporation of a ^{13}C-labeled, aromatic precursor L-dopa during melanization selectively labels aromatic polymers, while feeding exogenous ^{13}C-sugars highlights the alkyl, alkoxy, alkene, carboxylate, and amide groups (Figure 1e). These labeling schemes, used individually or in combination, allow the identification of an indole-based oligomeric structure for the melanin with putative associations with chitin as elucidated via many 2D ^{13}C–^{13}C DARR and COSY spectra.[40] Melanin is also found to undergo a progressive aromatization process in the cell wall. The versatile techniques of labeling and ssNMR have paved the way for investigating these supramolecular complexes of biopolymers that directly determine fungal pathogenicity.

Carbohydrates of Bacterial Biofilm and Microalgae

In bacteria, ssNMR has been employed to investigate the composition and structure of cell walls and their structural responses to antibiotics,[49–51] as well as the biofilm, an extracellular nanocomposite of cellulose and amyloid curli fibers.[41] Recently, Cegelski, Hengge, and coworkers have identified a chemically modified form of cellulose in *E. coli*, which is required for the assembly of the biofilm. This polymer has evaded high-resolution detection but is now picked up by the ^{13}C{^{31}P} REDOR technique, with the major dephasing of intensities happening (ΔS) to the carbon sites that are spatially proximal to the phosphate group (Figure 1f).[41] The genetic basis and molecular signaling involved in introducing this novel structure have also been elucidated.

Similar to plants, algae are another important photosynthesis biosystem with a high content of polysaccharides. Marcotte and coworkers have measured a model microalgae *C. reinhardtii*. With the dynamical filtering by multiple polarization methods, such as INEPT, heteronuclear NOE, CP, and single pulse, the signals from membrane galactolipids, structural carbohydrates in cell walls, and the storage polysaccharide starch are unambiguously selected and assigned in 1D/2D ^{13}C spectra.[52,53] They also identified the major crystalline form of amylose in the starch of microalgae and compared it with other crystalline forms obtained from various organisms.[54]

What Could MAS-DNP Contribute to Cell-wall NMR?

Selective Detection of the Porous and Outermost Cell Walls

The cell wall is a suitable system for MAS-DNP studies as this outer shell is easily selected over the intracellular components, and uniform polarization throughout the cell wall can be achieved after sample optimization. Hediger and coworkers have first revealed that the biradical TOTAPOL mainly accumulates in the bacterial cell walls of *B. subtilis*, which allows them to preferentially detect the cell-wall component and identify the optimal concentration of radicals for obtaining satisfactory resolution and sensitivity.[51] Bardet, Luterbacher, and coworkers have further shown that maximally 40–200 nm from the surface of poplar wood cell walls can be hyperpolarized via relayed DNP, which allows the selection of secondary cell walls over the inner middle lamellae.[55] Consistently, we have demonstrated that the microscopically porous plant materials (interfibrillar space of ~20–40 nm for primary cell walls) can easily accommodate the small biradicals (e.g., 1.3 nm across for

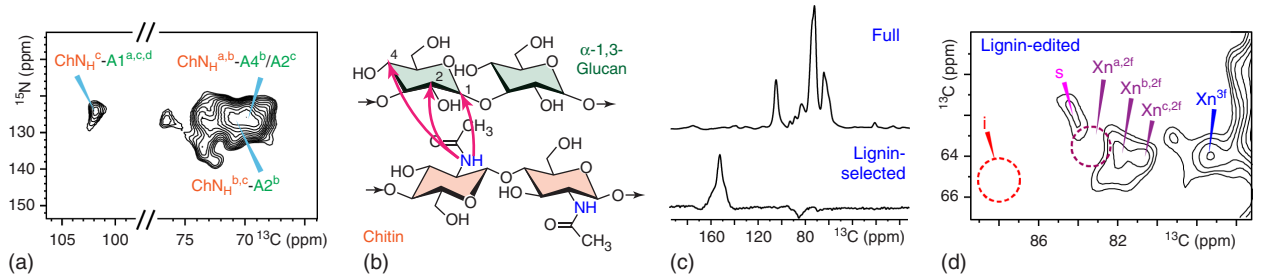

Figure 2. Polymer interface viewed by MAS-DNP. (a) A difference spectrum between two ^{15}N–^{13}C 2D spectra that were measured with a long (3 s) and short (0.1 s) ^{13}C–^{13}C PDSD mixing. Only intermolecular cross peaks are present in the difference spectrum. (b) Illustration of chitin–glucan packing discovered by the spectrum in panel (a). (c) Selection of lignin aromatics against carbohydrates. (d) Lignin-edited 2D spectra reveal the composition of lignin-bound carbohydrates. Dashed line circles show the carbohydrate components that lack interactions with lignin.[22,39]. ((a) Kang, X., Kirui, A., Muszyński, A., Widanage, M. C. D., Chen, A., Azadi, P., Wang, P., Mentink-Vigier, F., Wang, T. (2018). Molecular architecture of fungal cell walls revealed by solid-state NMR. Nature Communications, 9(1). doi:10.1038/s41467-018-05199-0. Public Domain; (b) Kang, X., Kirui, A., Muszyński, A., Widanage, M. C. D., Chen, A., Azadi, P., Wang, P., Mentink-Vigier, F., Wang, T. (2018). Molecular architecture of fungal cell walls revealed by solid-state NMR. Nature Communications, 9(1). doi:10.1038/s41467-018-05199-0. Licensed under CCBY 4.0; (c,d) Kang, X., Kirui, A., Dickwella Widanage, M. C., Mentink-Vigier, F., Cosgrove, D. J., & Wang, T. (2019). Lignin-polysaccharide interactions in plant secondary cell walls revealed by solid-state NMR. Nature Communications, 10(1). Licensed under CCBY 4.0)

AMUPol) to achieve a homogeneous polarization across the material, which has been confirmed by the identical spectral patterns measured with and without microwave irradiation.[33] A video protocol and the optimized procedures have been published to guide the preparation of samples that ensure a homogeneous distribution of radicals in the cell-wall region of whole-cell samples and efficient polarization of the cell-wall molecules.[56]

Detection of the Polymer Interaction Interface Involving Lowly Populated Molecules

The weak intensities of intermolecular cross peaks, due to the small dipolar couplings for long-range correlations and the relaxations occurring during the mixing period, have placed an obstacle to structural determination. The naturally low sensitivity is further worsened by multiple structural factors: (i) the dominance of water (50–80 wt%) in whole cells substantially reduces the effective volume of biomolecules, (ii) the coexistence of many polymers decreases the relative concentration of the molecules of interest, and (iii) certain molecules involved in the intermolecular interface have low abundance in cell, for example, chitin in *A. fumigatus* (accounting for ~10–15 wt% of the dry mass of cell walls) and lignin in the secondary cell walls of maize.[22,39] Despite the low concentration, these molecules are often of high significance to the mechanical and physical properties of cell walls, for example, chitin is the only partially crystalline polysaccharide in fungi and lignin–carbohydrate interactions waterproof and strengthen the plant biomass. Therefore, a feasible technique for elucidating their intermolecular packing has become a necessity.

These technical barriers can be overcome by integrating the sensitivity enhancement of MAS-DNP with the resolution improvement from spectral-editing techniques, which enables efficient detection of intermolecular contacts. We have recently demonstrated this strategy using the following examples. First, in *A. fumigatus*, long-range ^{15}N–^{15}N PAR spectrum has revealed extensive cross peaks between the amide signals from different chitin conformers, confirming the coexistence of these conformers in the same microfibril.[22] This is impressive considering that the nucleus being manipulated has worse sensitivity than ^{13}C, the experimental scheme is sensitivity challenging, and the interresidue correlations occur only between the chitin conformers that account for <10 wt% of the hydrated material. Second, the spectral subtraction of two parent ^{15}N–^{13}C correlation spectra measured with long and short ^{13}C–^{13}C mixing times has unambiguously resolved multiple cross peaks between the nitrogen of chitin amide and the carbons of α-1,3-glucans (Figure 2a,b). Notably, in order to subtract two spectra measured with different mixing times, a constant-time experimental scheme is often required at ambient temperature in order to compensate for the heterogeneous relaxations of rigid and mobile molecules during the mixing period,[32] but it is not needed at the cryogenic temperature of DNP at which longitudinal relaxation becomes uniformly long for most structural molecules. Third, with dipolar and frequency filters, as well as the microwave gating achieved through a mechanical shutter,[57] the weak signals of lignin are efficiently selected against the polysaccharide peaks that are 260-fold stronger (Figure 2c). This allows us to measure lignin-edited spectra to detect the carbohydrate components in close spatial proximity to these aromatics, which discovers that the threefold twisted xylan (Xn^{3f}) associates with lignin, while the extended flat-ribbon form ($Xn^{a,2f}$) lacks such binding (Figure 2d).

Skip the Labeling: Natural-abundance Investigations of Unlabeled Biomaterials

In addition to the assistance in structural analysis, MAS-DNP has also presented an exciting opportunity that could substantially expand the territory of carbohydrate NMR. This is achieved by enabling high-resolution characterization of unlabeled biomaterials utilizing the sensitivity boost from DNP. The typical sensitivity enhancement ($\varepsilon_{on/off}$) factors for

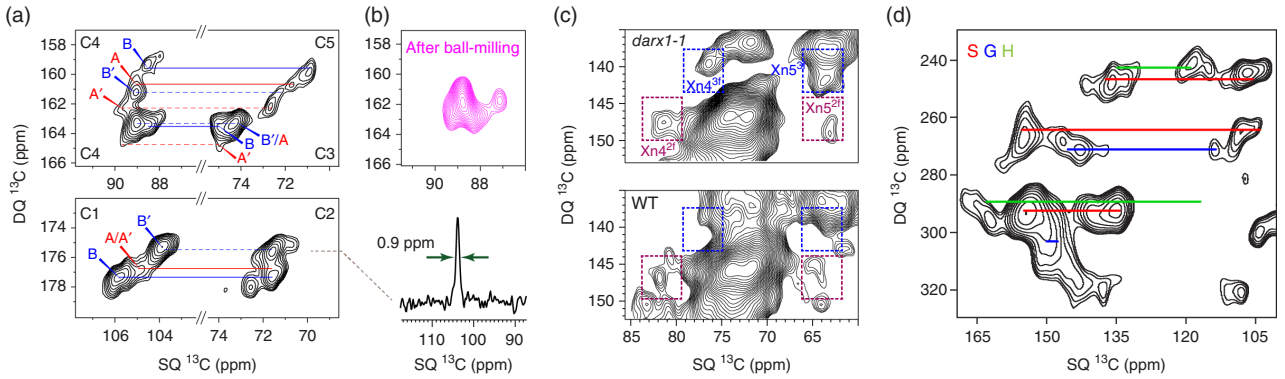

Figure 3. Natural-abundance DNP of cellulose, matrix polysaccharides, and lignin in plant biomass. (a) Natural-abundance 2D ^{13}C–^{13}C INADEQUATE spectrum of cellulose in unlabeled cotton. A and A′ indicate the glucose units in Iα cellulose allomorph, while B and B′ are glucose units in Iβ allomorph. 1D ^{13}C cross section extracted at $\omega_1 = 175$ ppm shows the ^{13}C linewidth of 0.9 ppm. (b) C4 region of the crystalline cellulose in cotton after 2 h of ball milling. (c) Resolved signals for twofold (purple) and threefold (blue) xylan in the stems of wild-type rice and its mutant. (d) Lignin regions of refocused INADEQUATE of wild-type poplar. S, H, and G indicate three fundamental units of lignin. Panels (a–c) were measured on a 600 MHz/395 GHz DNP, and panel (d) was collected on a 400 MHz/263 GHz DNP.[58–60] ((a,b) Kirui, A., Ling, Z., Kang, X., Dickwella Widanage, M. C., Mentink-Vigier, F., French, A. D., & Wang, T. (2018). Atomic resolution of cotton cellulose structure enabled by dynamic nuclear polarization solid-state NMR. Cellulose. doi:10.1007/s10570-018-2095-6. © 2018 Springer Nature; (c) Zhang, L., Gao, C., Mentink-Vigier, F., Tang, L., Zhang, D., Wang, S., Cao, S., Xu, Z., Liu, X., Wang, T., Zhou, Y., Zhang, B. (2019). Arabinosyl Deacetylase Modulates the Arabinoxylan Acetylation Profile and Secondary Wall Formation. The Plant Cell, 31 (5) 1113–1126. © 2019. Reprinted with permission from American Society of Plant Biologists; (d) Perras, F. A., Luo, H., Zhang, X., Mosier, N. S., Pruski, M., & Abu-Omar, M. M. (2017). Atomic-Level Structure Characterization of Biomass Pre- and Post-Lignin Treatment by Dynamic Nuclear Polarization-Enhanced Solid-State NMR. The Journal of Physical Chemistry A, 121(3), 623–630. doi:10.1021/acs.jpca.6b11121. © 2017 American Chemical Society)

cell-wall biomaterials are ~30-fold on the 600 MHz/395 GHz MAS-DNP spectrometers[22,39] and ~70-fold on the lower field (e.g., 400 MHz/263 GHz DNP).[58] The tremendous timesaving makes it feasible to measure 2D correlation spectra using the very low natural abundance of NMR-active isotopes, 1.1% for ^{13}C and 0.4% for ^{15}N, in unlabeled biomaterials.

Recently, we have optimized a protocol for preparing ssNMR/DNP samples using labeled or unlabeled materials.[56] Starting from this protocol, we have investigated the structure of both microcrystalline carbohydrates (cellulose) and disordered matrix polysaccharides (xylan) in intact plant stems or biomaterials, without isotope labeling.[59,60] A matrix-free protocol[61,62] is used to maximize the efficient volume of biomolecules, and 2D ^{13}C–^{13}C INADEQUATE spectra are collected within 5–9.5 h for each cotton sample and 17–37 h for each of the more complicated, rice stems. The ^{13}C resolution of the partially crystalline cellulose in cotton is largely retained at 100 K, with narrow ^{13}C linewidths of 0.9 ppm on a 600 MHz/395 GHz DNP system (Figure 3a).[59] As a result, the carbon connectivities of four magnetically nonequivalent glucose units in cellulose can be fully resolved, and we have further revealed that the ball-milling process, a standard procedure widely used in solution-NMR studies, has totally destroyed the native structure of cellulose microfibrils as evidenced by the distinct spectra (Figure 3b). In contrast, the ^{13}C linewidth for the mobile matrix polysaccharides has been broadened at low temperature due to the restriction of molecular motions that are important for averaging out the conformational distribution of these disordered molecules. Fortunately, we are still capable of resolving at least the flat-ribbon conformer and the twisted form of xylan in rice stems.[60] We have shown that, compared to the wild-type rice, a *darx1* mutant has dramatically increased the content of nonflat threefold xylan but reduced the relative amount of the flat-ribbon twofold xylan that associates with cellulose surface, revealing how this mutation perturbs xylan–cellulose interactions on the molecular level (Figure 3c).

In addition, Pruski, Abu-Omar, and coworkers have elucidated the lignin composition of poplar biomass: natural-abundance DNP enables the identification of various lignin subunits (Figure 3d, *p*-hydroxyphenyl, H; guaiacyl, G; and syringyl, S) and their complex linkages in catalytically processed and genetically engineered poplar species (with high or low content of S-units).[58]

Notably, Dr. De Paëpe and coworkers have demonstrated that long-range intermolecular correlations, with distances up to ~7 Å, can be detected using natural-abundance DNP, and this method is employed to probe π-stacking of the nanoassemblies formed by a cyclic diphenylalanine peptide.[63] They have also demonstrated the feasibility of measuring natural-abundance 2D ^{13}C–^{15}N correlation spectra on small organic molecules.[64,65] As dipolar truncation is no longer an issue at natural isotopic abundance, pulse sequences that efficiently recouple homonuclear (e.g., S3) or heteronuclear (e.g., TEDOR) dipolar couplings start to play a critical role in the structural determination of unlabeled molecules.[66–68] These technical advances have presented a unique opportunity for further exploring the structure of nitrogenated carbohydrates and intermolecular packing in unlabeled cells, which will be facilitated by the development of better radicals, for example, the AsymPolPOK that shortens DNP buildup time,[69,70] and more efficient polarizing mechanisms for high-field DNP at 800 MHz/527 GHz or above.[71–73]

Conclusions

High-resolution ssNMR of complex carbohydrates and cell-wall biomaterials is exactly at a turning point where high-resolution, large-scale investigations just became possible. The combination of various isotope-labeling schemes, a complete set of $^{13}C/^{15}N$-based techniques, and sensitivity enhancement from DNP has completed the toolbox and enabled many studies of cell walls and biomaterials in plants, fungi, bacteria, and algae. Since polysaccharides are significantly underinvestigated, there are many unresolved questions in this field. In addition, the development of natural-abundance DNP methods has eliminated the difficulty and expenses associated with isotope labeling, allowing us to investigate a large variety of biomaterials. Besides these highlights, there are many other advances in the field that could substantially facilitate carbohydrate ssNMR research such as database and software development,[23] proton detection under ultrafast MAS,[74,75] and the materialization of ultrahigh-field magnets. We hope this article could encourage more NMR colleagues to join the ongoing efforts in unveiling the function–structure relationship of polysaccharides and cell-wall architecture, which will, on the molecular level, guide the rationale development of advanced technologies to produce better biorenewable energy, biomaterials, antibiotics and antifungal agents, and other high-value products based on carbohydrates or their complex with other biomolecules.

Acknowledgments

This work was supported by National Science Foundation through NSF MCB-1942665. Tuo Wang thanks the support of the Center for Lignocellulose Structure and Formation, an Energy Frontier Research Center funded by the US Department of Energy, Office of Science, Basic Energy Sciences under award number DE-SC0001090 for research on plant cell walls. FMV and the National High Magnetic Field laboratory (NHMFL) is funded by the National Science Foundation Division of Materials Research (DMR-1157490 and 1644779), the State of Florida, and the NIH P41 GM122698.

Biographical Sketches

Liyanage D. Fernando, b. 1992. BS, 2017, University of Colombo, Sri Lanka. Her PhD research at Louisiana State University, supervised by Dr. Tuo Wang, focuses on the ssNMR and DNP studies for understanding the structural diversity of carbohydrates in fungal pathogens.

Wancheng Zhao, b. 1989. BS, 2011, Jilin University, China; MSc, 2017, under the supervision of Dr. Tiancheng Mu at Renmin University, China. His PhD research at Louisiana State University, under the mentorship of Dr. Tuo Wang, focuses on database development and the elucidation of plant cell-wall structure.

Malitha C. Dickwella Widanage, b. 1991. BS, 2015, University of Colombo, Sri Lanka; His PhD research at Louisiana State University is focused on the structural effects of antifungal drugs on fungal cell walls and the structural origin of drug resistance.

Frédéric Mentink-Vigier, b. 1984. MSc, 2008, Ecole Nationale Supérieure de Chimie ParisTech, France; PhD, 2011, Ecole Nationale Supérieure de Chimie ParisTech, France, under the supervision of Dr. L. Binet. He undertook two postdoctoral stays, first at the Weizmann Institute, Israel, with Profs. D. Goldfarb and S. Vega and then back in France at CEA Grenoble (Dr. Gaël De Paëpe). Since 2016, he holds a research faculty position at the National High Magnetic Field Laboratory to continue his research in DNP methodology, including new radical design.

Tuo Wang, b. 1988. BS, 2010, Nankai University, China; PhD, 2016, Massachusetts Institute of Technology, under the supervision of Dr. Mei Hong. He conducted postdoctoral research in Dr. Mei Hong's group at MIT and joined the faculty of the Chemistry Department at Louisiana State University in 2017, where he focuses on the structural elucidation of complex carbohydrates and other biomolecules. He was the recipient of Ralph E. Powe Junior Faculty Enhancement Award in 2019, DOE Early Career Award in 2020, and NSF Faculty Early Career Award in 2020.

Related Articles

Glycoproteins and Antibodies: Solution NMR Studies; Carbohydrates and Glycoconjugates; MAS-DNP Enhancements: Hyperpolarization, Depolarization, and Absolute Sensitivity

References

1. R. H. Atalla and D. L. Vanderhart, *Science*, 1984, **223**, 283.
2. M. C. Jarvis and D. C. Apperley, *Plant Physiol.*, 1990, **92**, 61.
3. A. N. Fernandes, L. H. Thomas, C. M. Altaner, P. Callow, V. T. Forsyth, D. C. Apperley, C. J. Kennedy, and M. C. Jarvis, *Proc. Natl. Acad. Sci. U. S. A.*, 2011, **108**, E1195.
4. G. Hou, S. Yan, J. Trebosc, J. P. Amoureux, and T. Polenova, *J. Magn. Reson.*, 2013, **232**, 18.
5. G. De Paëpe, J. R. Lewandowski, A. Loquet, A. Bockmann, and R. G. Griffin, *J. Chem. Phys.*, 2008, **129**, 245101.
6. A. Lesage, C. Auger, S. Caldarelli, and L. Emsley, *J. Am. Chem. Soc.*, 1997, **119**, 7867.
7. M. Aluas, C. Tripon, J. M. Griffin, X. Filip, V. Ladizhansky, R. G. Griffin, S. P. Brown, and C. Filip, *J. Magn. Reson.*, 2009, **199**, 173.
8. C. Ader, R. Schneider, K. Seidel, M. Etzkorn, S. Becker, and M. Baldus, *J. Am. Chem. Soc.*, 2009, **131**, 170.
9. M. D. Gelenter, T. Wang, S. Y. Liao, H. O'Neill, and M. Hong, *J. Biomol. NMR*, 2017, **68**, 257.
10. T. Gullion and J. Schaefer, *J. Magn. Reson.*, 1989, **81**, 196.
11. I. Bertini, C. Luchinat, G. Parigi, and R. Pierattelli, *ChemBioChem*, 2005, **6**, 1536.
12. Q. Z. Ni, E. Daviso, T. V. Can, E. Markhasin, S. K. Jawla, T. M. Swager, R. J. Temkin, J. Herzfeld, and R. G. Griffin, *Acc. Chem. Res.*, 2013, **46**, 1933.
13. A. J. Rossini, A. Zagdoun, M. Lelli, A. Lesage, C. Coperet, and L. Emsley, *Acc. Chem. Res.*, 2013, **46**, 1942.
14. F. Mentink-Vigier, U. Akbey, H. Oschkinat, S. Vega, and A. Feintuch, *J. Magn. Reson.*, 2015, **258**, 102.
15. K. Schmidt-Rohr, K. J. Fritzsching, S. Y. Liao, and M. Hong, *J. Biomol. NMR*, 2012, **54**, 343.
16. J. K. Williams, K. Schmidt-Rohr, and M. Hong, *Solid State Nucl. Magn. Reson.*, 2015, **72**, 118.
17. M. Dick-Perez, Y. A. Zhang, J. Hayes, A. Salazar, O. A. Zabotina, and M. Hong, *Biochemistry*, 2011, **50**, 989.
18. T. J. Simmons, J. C. Mortimer, O. D. Bernardinelli, A. C. Poppler, S. P. Brown, E. R. de Azevedo, R. Dupree, and P. Dupree, *Nat. Commun.*, 2016, **7**, 13902.
19. O. M. Terrett, J. J. Lyczakowski, L. Yu, D. Iuga, W. T. Franks, S. P. Brown, R. Dupree, and P. Dupree, *Nat. Commun.*, 2019, **10**, 4978.

20. M. Dick-Perez, T. Wang, A. Salazar, O. A. Zabotina, and M. Hong, *Magn. Reson. Chem.*, 2012, **50**, 539.
21. T. Wang, A. Salazar, O. A. Zabotina, and M. Hong, *Biochemistry*, 2014, **53**, 2840.
22. X. Kang, A. Kirui, A. Muszynski, M. C. D. Widanage, A. Chen, P. Azadi, P. Wang, F. Mentink-Vigier, and T. Wang, *Nat. Commun.*, 2018, **9**, 2747.
23. X. Kang, W. Zhao, M. C. Dickwella Widanage, A. Kirui, U. Ozdenvar, and T. Wang, *J. Biomol. NMR*, 2020, DOI: 10.1007/s10858-020-00304-2.
24. T. Wang, P. Phyo, and M. Hong, *Solid State Nucl. Magn. Reson.*, 2016, **78**, 56.
25. P. Phyo, T. Wang, Y. Yang, H. O'Neill, and M. Hong, *Biomacromolecules*, 2018, **19**, 1485.
26. T. Wang, H. Yang, J. D. Kubicki, and M. Hong, *Biomacromolecules*, 2016, **17**, 2210.
27. T. Wang, O. Zabotina, and M. Hong, *Biochemistry*, 2012, **51**, 9846.
28. P. B. White, T. Wang, Y. B. Park, D. J. Cosgrove, and M. Hong, *J. Am. Chem. Soc.*, 2014, **136**, 10399.
29. T. Wang, Y. B. Park, D. J. Cosgrove, and M. Hong, *Plant Physiol.*, 2015, **168**, 871.
30. P. Phyo, T. Wang, S. N. Kiemle, H. O'Neill, S. V. Pingali, M. Hong, and D. J. Cosgrove, *Plant Physiol.*, 2017, **175**, 1593.
31. P. Phyo, T. Wang, C. W. Xiao, C. T. Anderson, and M. Hong, *Biomacromolecules*, 2017, **18**, 2937.
32. T. Wang, J. K. Williams, K. Schmidt-Rohr, and M. Hong, *J. Biomol. NMR*, 2015, **61**, 97.
33. T. Wang, Y. B. Park, M. A. Caporini, M. Rosay, L. H. Zhong, D. J. Cosgrove, and M. Hong, *Proc. Natl. Acad. Sci. U. S. A.*, 2013, **110**, 16444.
34. T. Wang, Y. N. Chen, A. Tabuchi, D. J. Cosgrove, and M. Hong, *Plant Physiol.*, 2016, **172**, 2107.
35. T. Zhang, Y. Z. Zheng, and D. J. Cosgrove, *Plant J.*, 2016, **85**, 179.
36. T. Zhang, D. Vavylonis, D. M. Durachko, and D. J. Cosgrove, *Nat. Plants*, 2017, **3**, 17056.
37. C. M. Lee, X. Chen, P. A. Weiss, L. Jensen, and S. H. Kim, *J. Phys. Chem. Lett.*, 2017, **8**, 55.
38. Y. Z. Zheng, X. Wang, Y. N. Chen, E. Wagner, and D. J. Cosgrove, *Plant Physiol.*, 2018, **93**, 211.
39. X. Kang, A. Kirui, M. C. Dickwella Widanage, F. Mentink-Vigier, D. J. Cosgrove, and T. Wang, *Nat. Commun.*, 2019, **10**, 347.
40. S. Chatterjee, R. Prados-Rosales, B. Itin, A. Casadevall, and R. E. Stark, *J. Biol. Chem.*, 2015, **290**, 13779.
41. W. Thongsomboon, D. O. Serra, A. Possling, C. Hadjineophytou, R. Hengge, and L. Cegelski, *Science*, 2018, **359**, 334.
42. R. Dupree, T. J. Simmons, J. C. Mortimer, D. Patel, D. Iuga, S. P. Brown, and P. Dupree, *Biochemistry*, 2015, **54**, 2335.
43. N. J. Grantham, J. Wurman-Rodrich, O. M. Terrett, J. J. Lyczakowski, K. Stott, D. Iuga, T. J. Simmons, M. Durand-Tardif, S. P. Brown, R. Dupree, M. Busse-Wicher, and P. Dupree, *Nat. Plants*, 2017, **3**, 859.
44. Z. H. Gan, I. Hung, X. L. Wang, J. Paulino, G. Wu, I. M. Litvak, P. L. Gor'kov, W. W. Brey, P. Lendi, J. L. Schiano, M. D. Bird, L. R. Dixon, J. Toth, G. S. Boebinger, and T. A. Cross, *J. Magn. Reson.*, 2017, **284**, 125.
45. J. P. Latge, *Mol. Microbiol.*, 2007, **66**, 279.
46. S. Chatterjee, R. Prados-Rosales, S. Frases, B. Itin, A. Casadevall, and R. E. Stark, *Biochemistry*, 2012, **51**, 6080.
47. J. Y. Zhong, S. Frases, H. Wang, A. Casadevall, and R. E. Stark, *Biochemistry*, 2008, **47**, 4701.
48. S. Chatterjee, R. Prados-Rosales, S. Tan, V. C. Phan, C. Chrissian, B. Itin, H. Wang, A. Khajo, R. S. Magliozzo, A. Casadevall, and R. E. Stark, *J. Biol. Chem.*, 2018, **293**, 20157.
49. J. A. Romaniuk and L. Cegelski, *Philos. Trans. R. Soc. B*, 2015, **370**, 20150024.
50. R. Nygaard, J. A. H. Romaniuk, D. M. Rice, and L. Cegelski, *Biophys. J.*, 2015, **108**, 1380.
51. H. Takahashi, I. Ayala, M. Bardet, G. De Paepe, J. P. Simorre, and S. Hediger, *J. Am. Chem. Soc.*, 2013, **135**, 5105.
52. A. A. Arnold, B. Genard, F. Zito, R. Tremblay, D. E. Warschawski, and I. Marcotte, *Biochim. Biophys. Acta*, 2015, **1848**, 369.
53. A. A. Arnold, J. P. Bourgouin, B. Genard, D. E. Warschawski, R. Tremblay, and I. Marcotte, *J. Biomol. NMR*, 2018, **70**, 123.
54. A. Poulhazan, A. A. Arnold, D. E. Warschawski, and I. Marcotte, *Int. J. Mol. Sci.*, 2018, **19**, 3817.
55. J. Viger-Gravel, W. Lan, A. C. Pinon, P. Berruyer, L. Emsley, M. Bardet, and J. Luterbacher, *J. Phys. Chem. C*, 2019, **123**, 30407.
56. A. Kirui, M. C. Dickwella Widanage, F. Mentink-Vigier, P. Wang, X. Kang, and T. Wang, *J. Vis. Exp.*, 2019, **144**, e59152.
57. T. Dubroca, A. N. Smith, K. J. Pike, S. Froud, R. Wylde, B. Trociewitz, J. Mckay, F. Mentink-Vigier, J. van Tol, S. Wi, W. Brey, J. R. Long, L. Frydman, and S. Hill, *J. Magn. Reson.*, 2018, **289**, 35.
58. F. A. Perras, H. Luo, X. Zhang, N. S. Mosier, M. Pruski, and M. M. Abu-Omar, *J. Phys. Chem. A*, 2017, **121**, 623.
59. A. Kirui, Z. Ling, X. Kang, M. C. Dickwella Widanage, F. Mentink-Vigier, A. D. French, and T. Wang, *Cellulose*, 2019, **26**, 329.
60. L. Zhang, C. Gao, F. Mentink-Vigier, L. Tang, D. Zhang, S. Wang, S. Cao, Z. Xu, X. Liu, T. Wang, Y. Zhou, and B. Zhang, *Plant Cell*, 2019, **31**, 1113.
61. H. Takahashi, S. Hediger, and G. De Paepe, *Chem. Commun.*, 2013, **49**, 9479.
62. H. Takahashi, D. Lee, L. Dubois, M. Bardet, S. Hediger, and G. De Paepe, *Angew. Chem. Int. Ed.*, 2012, **51**, 11766.
63. K. Marker, S. Paul, C. Fernandez-de-Alba, D. Lee, J. M. Mouesca, S. Hediger, and G. De Paepe, *Chem. Sci.*, 2017, **8**, 974.
64. K. Marker, M. Pingret, J. M. Mouesca, D. Gasparutto, S. Hediger, and G. De Paepe, *J. Am. Chem. Soc.*, 2015, **137**, 13796.
65. A. N. Smith, K. Marker, S. Hediger, and G. De Paepe, *J. Phys. Chem. Lett.*, 2019, **10**, 4652.
66. P. E. Kristiansen, M. Carravetta, W. C. Lai, and M. H. Levitt, *Chem. Phys. Lett.*, 2004, **390**, 1.
67. G. Teymoori, B. Pahari, B. Stevensson, and M. Eden, *Chem. Phys. Lett.*, 2012, **547**, 103.
68. C. P. Jaroniec, C. Filip, and R. G. Griffin, *J. Am. Chem. Soc.*, 2002, **124**, 10728.
69. F. Mentink-Vigier, I. Marin-Montesinos, A. P. Jagtap, T. Halbritter, J. van Tol, S. Hediger, D. Lee, S. T. Sigurdsson, and G. De Paepe, *J. Am. Chem. Soc.*, 2018, **140**, 11013.
70. F. Mentink-Vigier, *Phys. Chem. Chem. Phys.* 2020, **22** (6), 3643. https://doi.org/10.1039/C9CP06201G.
71. G. Mathies, M. A. Caporini, V. K. Michaelis, Y. P. Liu, K. N. Hu, D. Mance, J. L. Zweier, M. Rosay, M. Baldus, and R. G. Griffin, *Angew. Chem. Int. Ed.*, 2015, **54**, 11770.
72. K. Jaudzems, A. Bertarello, S. R. Chaudhari, A. Pica, D. Cala-De Paepe, E. Barbet-Massin, A. J. Pell, I. Akopjana, S. Kotelovica, D. Gajan, O. Ouari, K. Tars, G. Pintacuda, and A. Lesage, *Angew. Chem. Int. Ed.*, 2018, **57**, 7458.
73. F. Mentink-Vigier, G. Mathies, Y. Liu, A. L. Barra, M. A. Caporini, D. Lee, S. Hediger, R. G. Griffin, G. De Paepe, *NMR. Chem. Sci.* 2017, **8** (12), 8150. https://doi.org/10.1039/C7SC02199B.
74. P. Phyo and M. Hong, *J. Biomol. NMR*, 2019, **73**, 661.
75. C. Bougault, I. Ayala, W. Vollmer, J. P. Simorre, and P. Schanda, *J. Struct. Biol.*, 2019, **206**, 66.